18th International Conference
ENGINEERING MECHANICS 2012
Svratka, Czech Republic, May 14 – 17, 2012

pp. 513–521
Paper #60

MOTION OF ROTATING SPHERICAL PARTICLES TOUCHING A WALL

Z. Chára[*], P. Vlasák[**], I. Keita[***]

Abstract: *The paper deals with an analysis of motion of rotating spherical particle in calm water, when the particle is in contact with a smooth, horizontal wall. The motion was visualized by a fast digital camera at 1000 frames/second. Based on software analysis the particle trajectories as well as rotational velocities were determined. Values of vertical, horizontal and rotational velocities were used as input parameters for numerical model and the results are compared with experimental data. Experiments were performed with glass particle of diameter 25 mm, initial values of rotational speeds varied from 500 to 3000 revolution per minute.*

Keywords: ***Particle rotation, particle trajectory, Magnus force.***

1. Introduction

Particle motion and particle-wall collision play an important role in many industrial processes involving suspension flows. The collisions affect particle accumulation and dispersion and inter-phase transport and mixing. Compared to a dry collision the kinetic energy of a particle in a liquid environment is dissipated by viscous stresses in the liquid and by inelasticity during collision (Li et al., 2012). The ratio of particle inertia to viscous forces is quantified through the Stokes number, $St = (1/9)(\rho_p/\rho_f)Re$, where Re is the particle Reynolds number based on impact velocity. Barnocky & Davis (1988) experimentally examined the impact of a sphere on a surface covered by a thin layer of liquid to investigate the critical Stokes number. The work by Davis et al. (2002) also used a thin layer of liquid but they measured the impact and rebound velocity to determine the effective coefficient of restitution. Joseph et al. (2001) measured the approach and rebound of a fully immersed collision to determine the coefficient of restitution as function of the Stokes number. They showed that below a Stokes number of approximately 10 no rebound of the particle occurs and for a Stokes number grater than 1000 the particle rebound is not affected by the surrounding fluid. A lot of computational studies have also considered the problem of particle collision in a liquid. Leweke et al. (2004) computed the flow generated by a particle colliding normal to a surface without rebound. Their simulations showed the development of vortex rings around the particle.

Although many papers deal with the particle-wall collision a little is known about the collision when the particle rotates. The aim of this contribution is to analyze a movement of the rotating particle, calculate a theoretical trajectory of the particle and compare it with the experimental observation.

2. Experimental set-up

The experiments with rotating spherical particle were realized in a water tank of dimensions 40 x 28 x 20 centimeters. The tank was filled with water up to a level 60 mm above the bed. The bed was formed by a glass plate of thickness 19 mm. The particle was a glass sphere of diameter 25 mm and density 2470 kg/m^3. Water temperature was 24^{o}C. The sphere was sped up in a special spinning device situated above the water level. The sphere was held between cups and rotated about a horizontal axis

[*] Ing. Zdeněk Chára, CSc.: Institute of Hydrodynamics AS CR, v. v. i., Pod Paťankou 30/5; 166 12, Prague; CZ, e-mail: chara@ih.cas.cz

[**] prof. Pavel Vlasák, DrSc.: Institute of Hydrodynamics AS CR, v. v. i., Pod Paťankou 30/5; 166 12, Prague; CZ, e-mail: vlasak@ih.cas.cz

[***] Ibrahima Keita, PhD.: Institute of Hydrodynamics AS CR, v. v. i., Pod Paťankou 30/5; 166 12, Prague; CZ

with an initial angular velocity ω_0, which was measured by a tachometer. When the trigger was released, the springs pulled the cups apart, allowing the ball to fall freely in water. The spinning device ensured the required spherical rotation in the given plane and translational velocity of the ball was reached by free fall. The device allowed the sphere to spin up to 6 500 revolutions per minute (rpm), but in these experiments a range of 500-3000 rpm was used. Since the device was above water level the particle passed through the surface and this passing slightly modified its movement. Consequently even a non-rotating particle did not move only vertically but with some horizontal shift. After a collision with the bed, the particle rebounded and the combined translational and rotational motion continued.

The particle movement in water was recorded with a frequency of 1000 frames per second using a digital video camera NanoSence III+. Hairlines were drawn along two perimeters of the particle to make it possible to visualize the particle rotation. Only experiments in which the plane of the particle trajectory was parallel to the plane of the video camera objective were chosen.

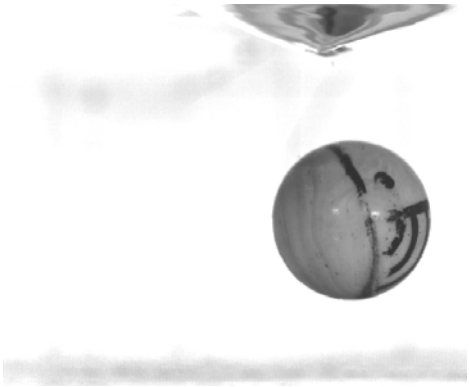

Fig.1: Original image taken from camera

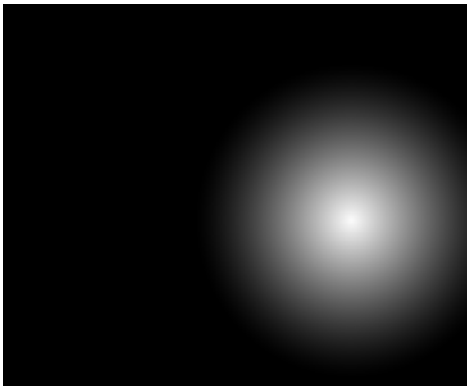

Fig.2: Convolution between 2D filter and original image

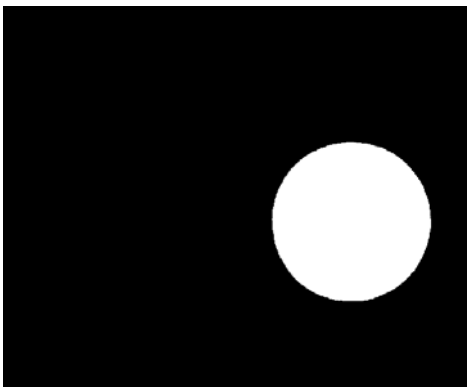

Fig.3: Particle shape after binary operation

Typical picture taken from the camera is shown in Fig. 1. To analyze the particle movements we applied functions implemented in Matlab Image Processing Toolbox. Firstly we chose a 2-D filter with circular shape and then we performed a convolution between the original image and the 2-D filter. The result is shown in Fig. 2, where the maximum white intensity corresponds to the particle centre. Even if the original image has a relatively high scale factor (13.6 pixels/mm) the trajectory based on the image pixels is inaccurate (see Fig. 4). Fig. 4 shows both the trajectories and the vertical velocities calculated from the particle trajectories. As can be seen in Fig. 4 using only pixels resolution to determine the velocity lets to enormous errors. To improve the resolution of the image we applied a fitting of the white intensity in the convolution image (Fig. 2). In both vertical and horizontal direction we used a polynominal curve of the fifth degree to approximate the white intensity. And we suppose that the position of the particle centre corresponds to the maximum of the white intensity. This way seems to give much better results compared with previous one. Another possibility how to improve the particle center identification is to convert the original image into binary one, (Fig. 3), and on this image perform some binary operations. This approach gives the best results, (Fig. 4), but constant conditions regarding the image contrast are required. If we know a position of the particle center the translational velocity components can be easily calculated.

The rotational velocities were determined from the following idea. The spherical particle was marked by two lines (like meridian and equator) which form two planes going through the centre of the particle (point C). In each time step we chose arbitrarily two points (A,B) on the equator (or meridian) and looked for a normal vector of the plane (ACB). If time series of the normal vectors is known, the 2D rotational velocity can be calculated.

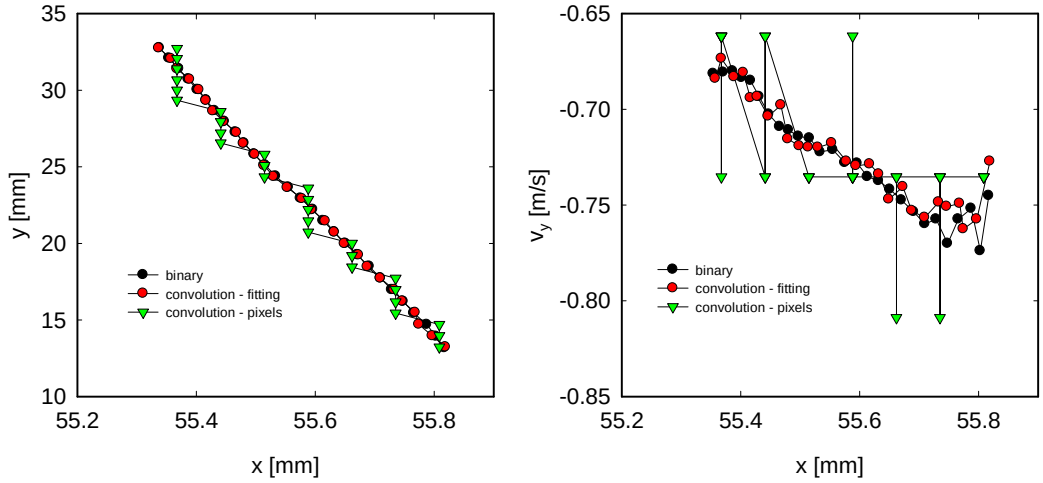

Fig.4: Comparison of different ways of particle location (left-trajectory, right –vertical velocity)

3. Discussion of the results

The particle motion in fluids is described by a set of ordinary differential equations taking into account interaction of several forces like submerged gravitational force, drag force, force due to the added mass, Magnus and history forces and torque acting on a rotating particle. History force was not considered due to the relatively large particle diameter and high Reynolds number (Re > 6000) in a vicinity of the wall. So, the system of the equations was considered in the following form

$$\begin{aligned} m\frac{d\vec{u}}{dt} &= \vec{F}_g + \vec{F}_d + \vec{F}_m + \vec{F}_M, \\ I\frac{d\vec{\omega}}{dt} &= \vec{M} \end{aligned} \tag{1}$$

where $\boldsymbol{m}$ is particle weight, $\boldsymbol{F_g}$, $\boldsymbol{F_d}$, $\boldsymbol{F_m}$ and $\boldsymbol{F_M}$ are gravitational, drag, added mass and Magnuse forces respectively. $\boldsymbol{I}$ is the particle momentum of inertia, $\boldsymbol{\omega}$ is rotational velocity and $\boldsymbol{M}$ is the drag torque given by the formula

$$\vec{M} = -C_\omega \frac{\rho_f}{2} \vec{\omega} |\vec{\omega}| r^5 \tag{2}$$

where C_ω is dimensionless drag torque coefficient. The reliable experimental and theoretical data of the coefficient C_ω are described by Sawatzki (1970). The drag force was determined by the following expression

$$\vec{F}_d = \left[\frac{24}{Re} \left(1 + 0.15\, Re^{0.687} \right) \right] \left(\rho_f / 2 \right) \pi (d/2)^2 \vec{u} |\vec{u}| \tag{3}$$

and Magnus force was given as

$$\vec{F}_M = C_M \frac{\pi d^3}{6} \rho_f \left[\vec{\omega} \times \vec{u} \right] \quad \left(= \frac{C_{LR}}{\Gamma} \frac{\pi d^3}{16} \rho_f \left[\vec{\omega} \times \vec{u} \right] \right) \tag{4}$$

where C_M is the dimensionless Magnus force coefficient. In the bracket there is another expression for Magnus force which can be found in literature and where the lift coefficient is used instead the Magnus force coefficient ($C_{LR} = 8\Gamma/3\ C_M$). Γ is dimensionless parameter sometimes called as dimensional angular velocity ($\Gamma = 2Re_\omega/Re$). The theoretical analysis of the Magnus force was performed by Rubinov & Keller (1961) for very small values of the Reynolds numbers and they deduced $C_M = 0.75$. In the range of moderate Reynolds numbers ($550 < Re < 1600$, $\Gamma < 0.7$) Tsuji et al. (1985) observed trajectories of a sphere which collided with an inclined plate submerged in water and they suggested $C_M = 0.15 \pm 0.04$. Oesterle & Dinh (1998) proposed the following formula for the lift coefficient ($10 < Re < 140$, $1 < \Gamma < 7$)

$$C_{LR} = 0.45 + \left(2\Gamma - 0.45 \right) \exp\left(-0.075\, \Gamma^{0.4}\, Re^{0.7} \right), \quad Re < 140 \tag{5}$$

In our experiments the range of Reynolds numbers was from 1000 to 20 000 and the range of non-dimensional angular velocity from 0.5 to 10. As was mentioned above the particle trajectories were used to calculate the vertical as well as the horizontal velocity components. Time resolution was given by the camera frame rate and for all tested cases $\Delta t = 0.001$ sec. First of all we analyzed the angular velocities and the results we compared with particle drag torque to determine the coefficient of drag torque, C_ω. Fig 5 shows time series of the measured angular velocities for the initial values of rotational velocities – 500, 1000, 2000 and 3000 rpm. The particle always rotated in counter-clockwise direction.

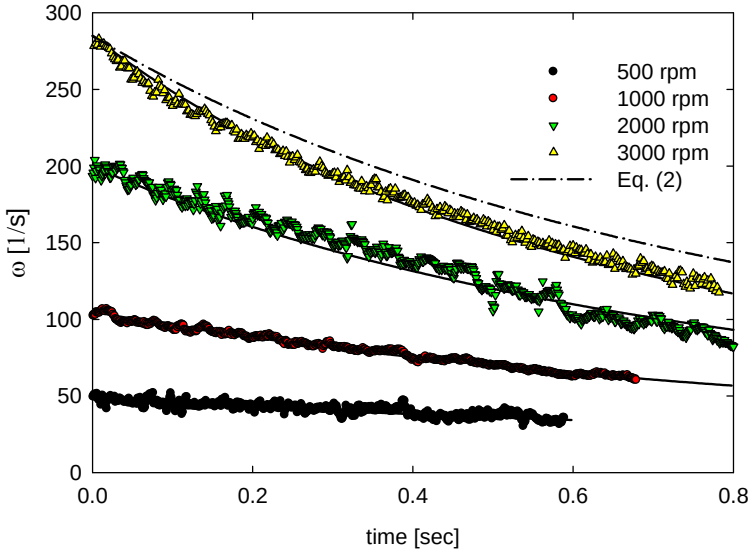

Fig.5: Time series of angular velocities

As can be seen in Fig. 5 the angular velocities monotonically decrease in time which means that negligible changes of angular velocities occurred during particle-bed collisions (at least the changes

lay in a range of experimental errors). We approximated the data of angular velocities by the Equation (2) with the coefficient of drag torque taken directly from Sawatzki (1970) data. The approximation is shown as a dash-dot line in Fig. 5 and in a whole range of time interval the line is above the experimental data. To get a better approximation (solid lines in Fig. 5) the drag torque coefficient is suggested to be slightly modified according to the formula

$$C_{\omega} = 1.3\ C_{\omega\ Sawatzki} \tag{6}$$

The aim of this paper is to analyze the particle trajectories and with help of equation set (1) calculate the trajectories with initial values of both translational and rotational velocities taken from the experiments. Figs. 6, 7 and 8 show particle trajectories for the non-rotating particle and for the particle with rotation 1000 and 3000 rpm. The left part of the figures show time series of the vertical particle position, the right part shows the particle positions in the *x*-*y* plane (***x*** is horizontal coordinate and goes from left to right, ***y*** is vertical coordinate and goes from bottom to upwards). The interruption of the trajectory for the non-rotating particle is due to a relatively small water depth. When the particle went up after the first collision with the bed, the particle nearly touched a water level and when the particle started again to settle a part of the water level was pulled down. Since the non-rotating particle had a small but not a negligible value of horizontal velocity it moved along the bottom (see Fig. 6, right). The initial trajectory of the rotating particle is going down from the left to the right do to the counter-clockwise rotation and hence due to the Magnus force. Depending on the angle of the first trajectory the particle either reversed its movement immediately after the first collision, (Fig. 7, right), or continued forward and reversed after the second collision, (Fig. 8, right).

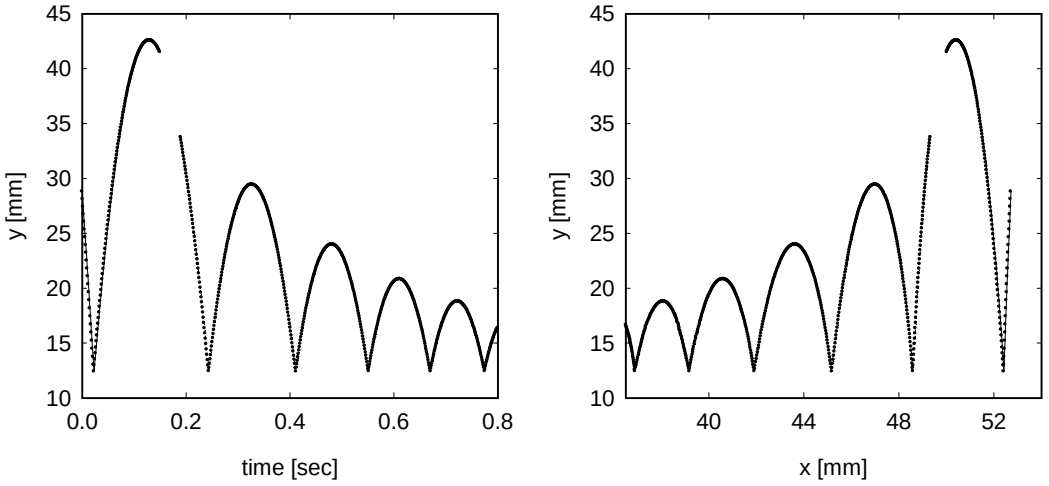

Fig.6: Trajectories of non-rotating particle

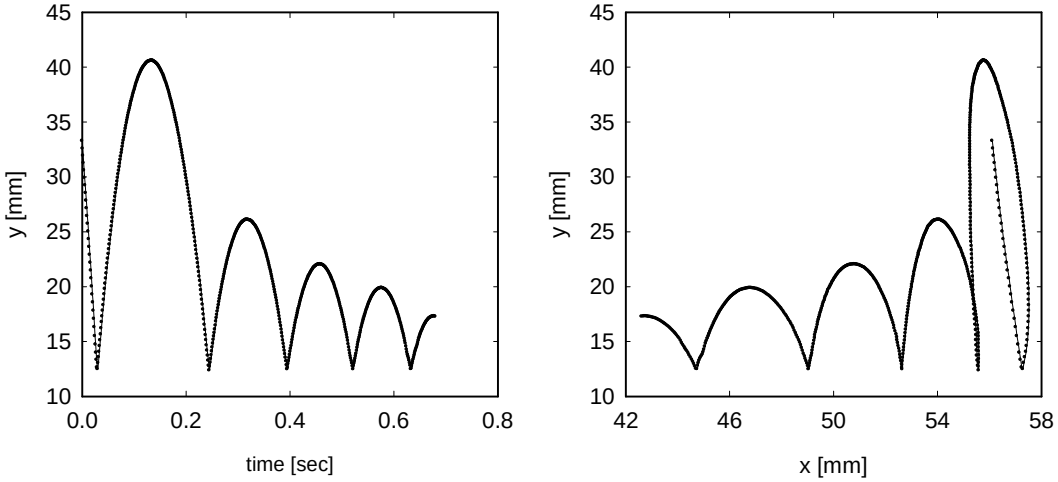

Fig.7: Trajectories of rotating particle with initial rotation 1000 rpm

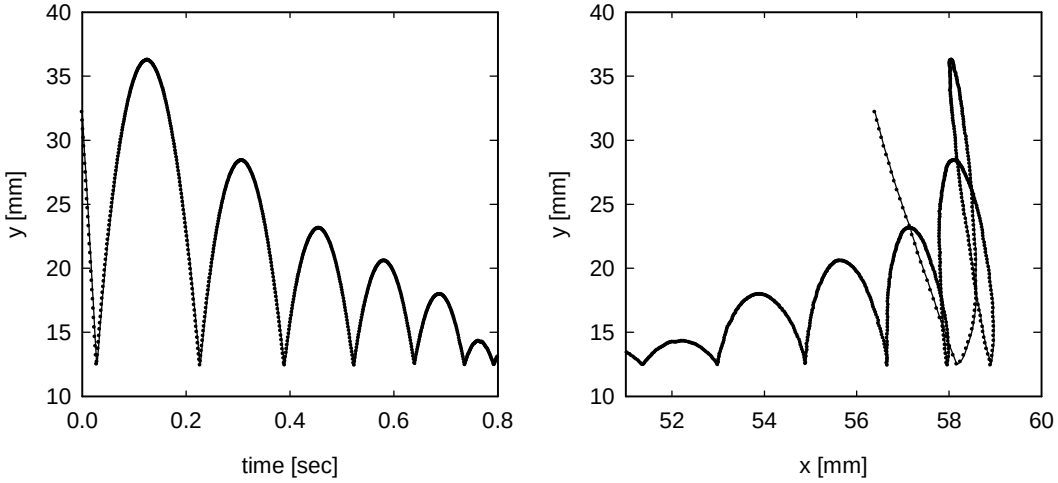

Fig.8: Trajectories of rotating particle with initial rotation 3000 rpm

Figs. 9, 10 and 11 show the translational particle velocities determined from trajectories of the particle center. Blue lines in these figures show the velocities in horizontal direction, red lines show the vertical velocity component. While the vertical velocities changed for a very short time during the collision process, somewhat different behavior was observed for the horizontal velocities in the case of rotating motion. The horizontal velocities increased and just before the collision they decreased. After the collision the horizontal velocities continued to decrease, but the time derivate of the horizontal velocity is much higher compared to the time derivate of the vertical velocities. This situation is clearer in Fig. 12 where a detail of time series of the first rebound is shown for initial rotation 1000 and 3000 rpm and for different angles of incoming trajectories. The angels are between the trajectories and a normal vector of the bed. The higher is the angle the higher is the horizontal velocity before the impact. The origin of time coordinate corresponds to the time of the collision. As can be seen in Fig. 12 the particle strongly accelerates in the horizontal direction just after the impact. The acceleration acts in direction of the Magnus force and it is restricted to a region close to the bed (up to a distance 0.2D). The acceleration depends on the initial conditions of rotation, the higher is the rotation, the higher is the acceleration.

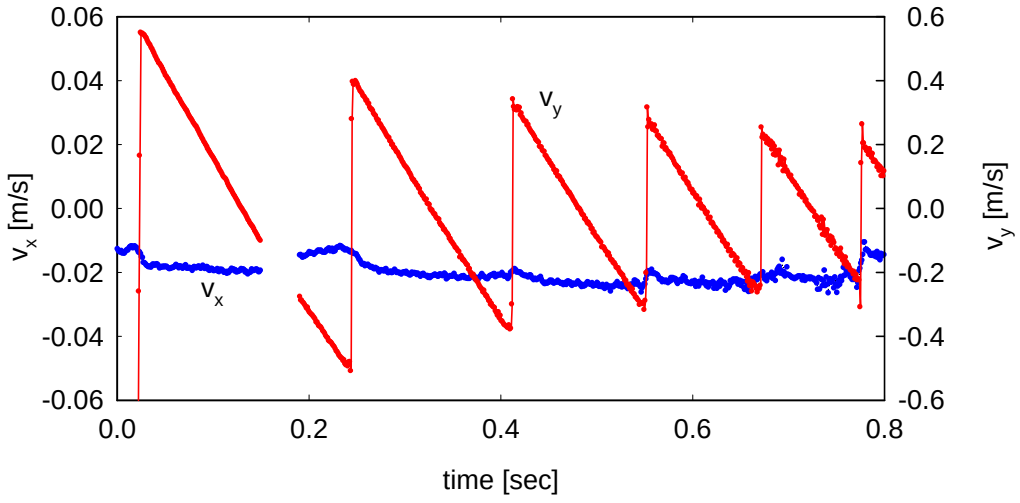

Fig.9: Translational velocities of non-rotating particle (blue - horizontal, red - vertical velocities)

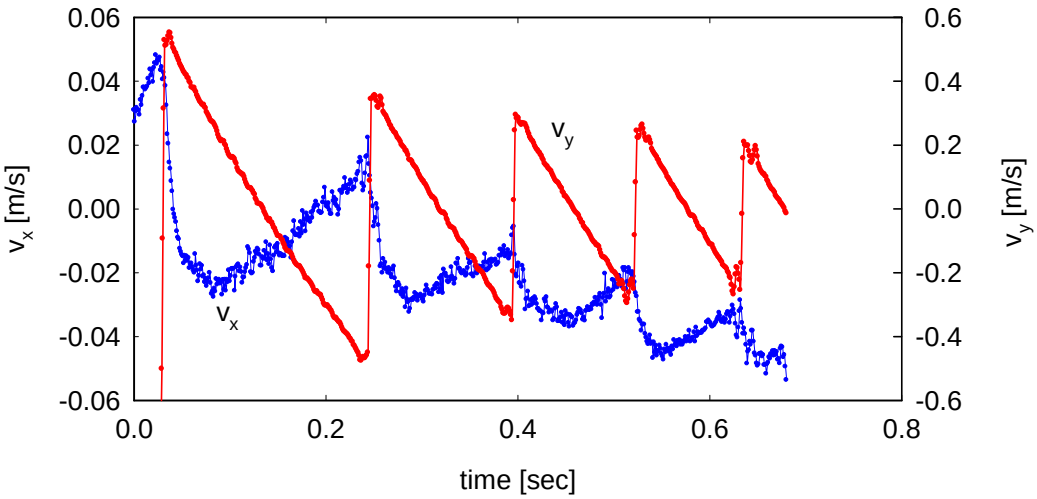

Fig.10: Translational velocities of rotating particle - 1000 rpm

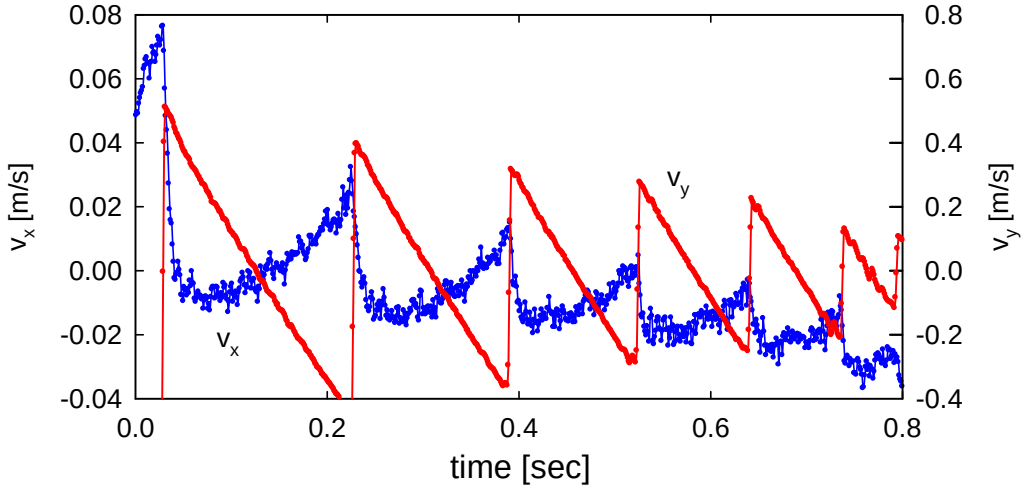

Fig.11: Translational velocities of rotating particle - 3000 rpm

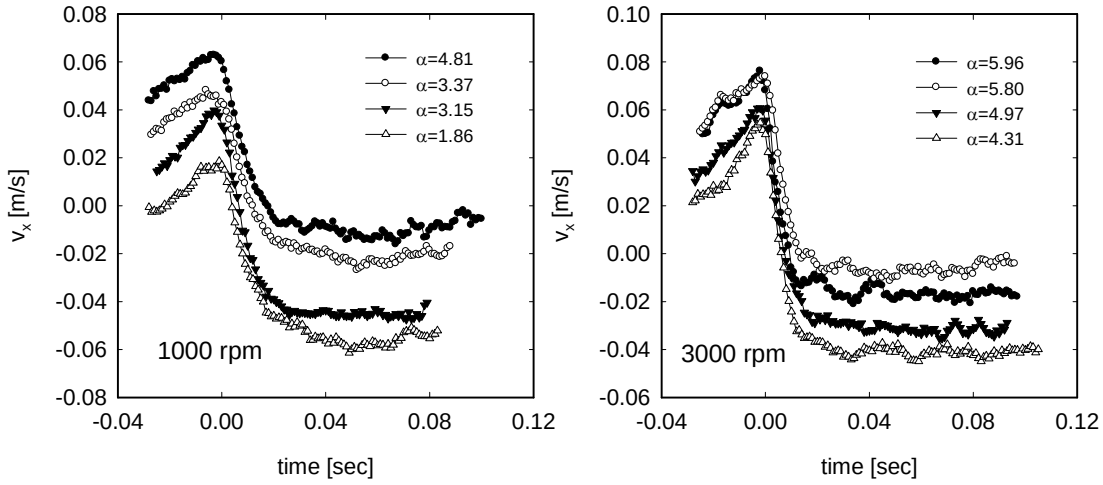

Fig.12: Horizontal velocity component of rotating particle after the first rebound

Another interesting feature can be concluded from the time series of the horizontal velocities and the vertical position of the particle. Between two impacts the particle quickly accelerates and then slowly decelerates but the point of transition does not correspond to the point where the particle

reaches the maximal position above the bottom and where the vertical velocity changes the direction. The point of transition precedes the maximal position of several tens of milliseconds.

As we know the particle trajectories and the translational and rotational velocities just after the impact and supposing that the Magnus force coefficient is constant over each individual jump we could solve the Equations (1). The Magnus force coefficient was determined for each jump to obtain the best coincidence between the measured and the calculated trajectories. Figs. 13 and 14 show calculated (red lines) and measured (blue lines) values of the particle trajectories and the translational velocities for a case of the initial rotation 1000 rpm.

All values of the Magnus force coefficients were plotted together versus initial values of the non-dimensional angular velocity Γ_0, ($\Gamma_0 = 2Re_{\omega out}/Re_{out}$). The results are shown in Fig. 15 and the Maguns force coefficient can be approximated by the equation

$$C_M = \frac{0.523}{3.49 + \Gamma_0} \tag{7}$$

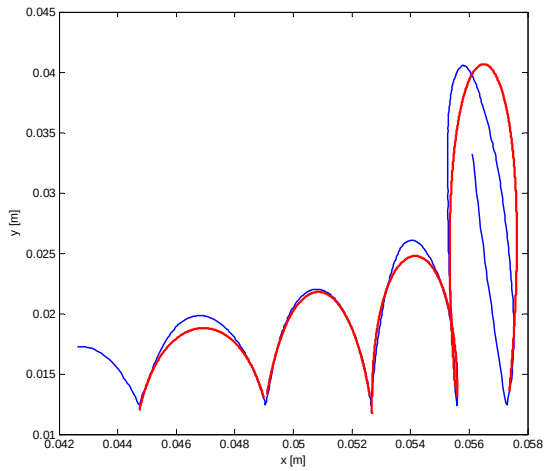

Fig.13: Comparison between calculated (red lines) and measured (blue lines) trajectories of rotating particle – 1000 rpm

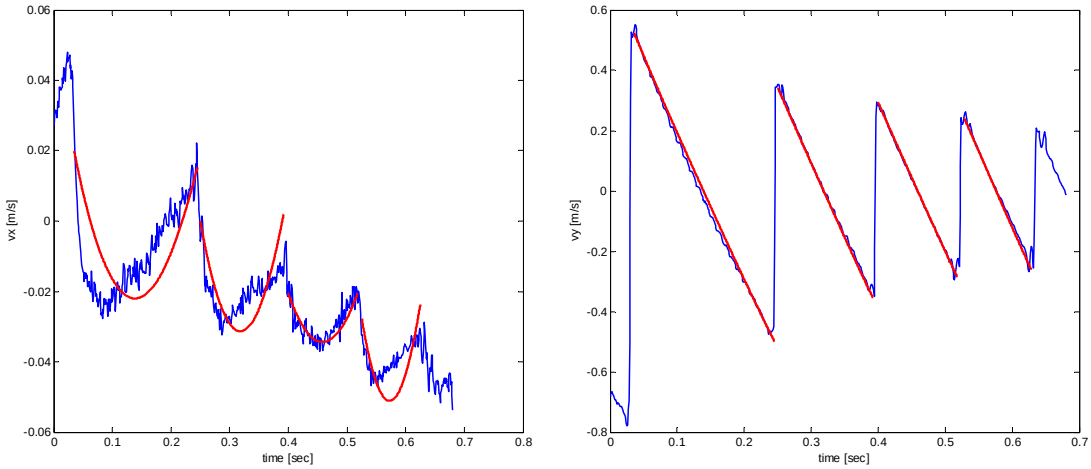

Fig.14: Comparison between calculated (red lines) and measured (blue lines) translational velocities of rotating particle – 1000 rpm

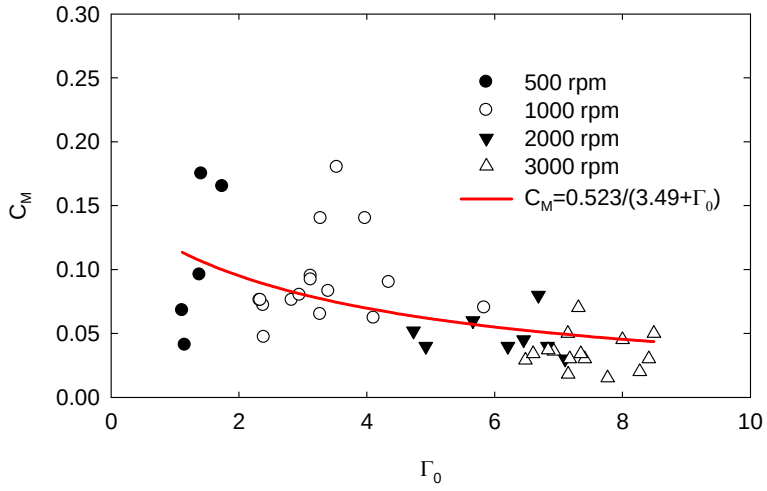

Fig.15: Dependence of Magnus force coefficients, (C_M), on initial values of non-dimensional angular velocities, (Γ_0)

4. Conclusion

Movements of the spherical particles rotating in calm water and touching the horizontal bed were visualized and analyzed. Due to very low values of dynamic friction coefficients no changes of the angular velocities were observed during collision process. The angular velocities monotonically decreased during time and the drag torque acting on the particle could be described by Equation (2) where a modification of the drag torque coefficient is suggested according to the Equation (6).

Measured values of translational and angular velocities just after the collision were used as initial parameters for numerical simulations of the particle movements. The Magnus force coefficients were determined for each jump to obtain the best coincidence between the measured and the calculated trajectories. The Magnus force coefficient can be approximated by the Equation (7).

Acknowledgement

The support under project No. 103/09/1718 of the Grant Agency of the Czech Republic and RVO: 67985874 is gratefully acknowledged.

References

Barnocky, G. & Davis, R.H. (1988) Elastohydrodynamics collision and rebound of sphere: experimental verification. *Phys. Fluids*, 31, pp. 1324-1329.

Davis, R.H., Rager, D.A. & Good, B.T. (2002) Elastohydrodynamic rebound of sphere from coated surface. *J. Fluid Mech*., 468, pp. 479-497.

Joseph, G.G., Zenit, R., Hunt, M.L. & Rosenwinkel, A.M. (2001) Particle-wall collisions in a viscous fluid. *J. Fluid Mech.*, 443, pp. 329-346.

Leweke, T., Thompson, M.C. & Hourigan, K. (2004) Vortex dynamics associated with the collision of a sphere with a wall. *Phys. Fluids* 16 (9), pp. 74-77

Li, X., Hunt, M.L. & Colonius T. (2012) A contact model for normal immersed collisions between a particle and a wall., *J. Fluid Mech.*, 691, pp. 123-145.

Oesterle, B. & Dinh, T.B. (1998) Experiments on the lift of a spinning sphere in the range if intermediate Reynolds numbers. *Experiments in Fluids*, 25, pp. 16-22

Rubinov, S.I. & Keller, J.B. (1961) The transverse force on a spinning sphere moving in a viscous fluid. *J. Fluid Mech*., 11, pp. 447-459.

Sawatski, O. (1970) Das Stromungsfeld um eine rotierende Kugel. *Acta Mechanica,* 9, pp. 159-214.

Tsuji, Y., Morikawa, Y. & Mizuno, O. (1985) Experimental measurements of the Magnus force on a rotating sphere at low Reynolds numbers. *ASME J. Fluid Eng.*, 107, pp. 484-488.